

Article

# Influence of Vibration Treatment and Modification of A356 Aluminum Alloy on Its Structure and Mechanical Properties

Vladimir V. Promakhov<sup>1</sup>, Marina G. Khmeleva<sup>1,\*</sup>, Ilya A. Zhukov<sup>1,2</sup>, Vladimir V. Platov<sup>1</sup>, Anton P. Khrustalyov<sup>1</sup>  and Alexander B. Vorozhtsov<sup>1,2</sup>

<sup>1</sup> National Research Tomsk State University, Lenin Av. 36, Tomsk 634050, Russia; vvpromakhov@mail.ru (V.V.P.); gofra930@gmail.com (I.A.Z.); vova.platov.85@mail.ru (V.V.P.); tofik0014@mail.ru (A.P.K.); abv1953@mail.ru (A.B.V.)

<sup>2</sup> Institute for Problems of Chemical and Energetic Technologies of the Siberian Branch of the Russian Academy of Sciences, Socialisticheskaya St. 1, Biysk 659322, Russia

\* Correspondence: khmelmg@gmail.com; Tel.: +7-913-861-22-45

Received: 13 December 2018; Accepted: 12 January 2019; Published: 15 January 2019



**Abstract:** A series of casting experiments was conducted with A356 aluminum alloys by applying vibration treatment and using Al-TiB<sub>2</sub> composite master alloys. The main vibration effects include the promotion of nucleation and a reduction in as-cast grain size. Using composite master alloys with titanium diboride microparticles allows further reduction in the average grain size to 140 μm. The reasons for this behavior are discussed in terms of the complex effect on the melt, considering the destruction of dendrites, and the presence of additional crystallization centers. Tensile tests were performed on the samples obtained during the vibration treatment and with titanium diboride particles. The tensile strength increased from 182 to 227 MPa after the vibration treatment for the alloys containing titanium diboride.

**Keywords:** aluminum; particles; master alloy; vibration treatment; mechanical properties

## 1. Introduction

Aluminum alloys are attracting the attention of researchers due to their wide application as structural materials in various industries, such as transport, aerospace, and construction. Of particular interest among the cast alloys based on aluminum are Al-Si system alloys, which are characterized by good mechanical and metallurgical properties [1]. Based on the classical concepts of mechanics and solid-state physics, the deformation and fracture of crystalline solids are the main phenomena that determine the behavior of materials under loads. The strain resistance of metallic materials in the solid state can be increased by using an alloy structure refinement [2,3]. In practice, the best-known methods for obtaining a fine-grained microstructure of cast aluminum alloys are (1) melt treatment using external fields (vibration [4–6], ultrasound [7,8], and electromagnetic stirring [9,10]); and (2) the use of grain refining master alloys [11–13].

Vibration treatment is one of the most cost-effective melt processing methods using external fields. As shown in some studies, the vibration treatment of metallic melts has a number of advantages, including degassing and the destruction of dendrites) [1,5,14,15]. Reducing the grain size was experimentally shown to increase with increasing vibration frequency up to a certain value [16]. This was confirmed by other studies [17–19].

Completely describing the mechanisms of elastic vibrations in a metallic melt and on the resulting crystal structure is difficult due to the variety of process parameters, such as vibration parameters, the volume of a test sample, melt properties, temperature, etc. [20–22]. However, the practical outcomes

have been reliably confirmed, including microstructure refinement, reduction, or complete elimination of columnar structure due to equiaxed crystal growth, refinement of dendrite arm spacing, improved plastic, and strength and special properties for metals and alloys [5,23]. The results of a case study on the influence of mechanical vibration parameters (frequency and amplitude) on the microstructure and mechanical properties of A356 aluminum alloy were presented by Kumar S. et al. [24]. The authors found that tensile strength, yield strength, and elongation were increased by 27%, 18%, and 52%, respectively. The effects of frequency and processing time on the size of the primary  $\alpha$ -Al solid phase and density of an A356 aluminum alloy were studied [14]. The maximum grain refinement occurred at a frequency of 50 Hz and a treatment time of 15 min, and the size of the  $\alpha$ -Al grains decreased to 173  $\mu\text{m}$ . Selivorstov V. et al. [25] concluded that the best mechanical properties were achieved after treating an A356 alloy at frequencies of 100 Hz and 150 Hz, and tensile strength and yield strength increased by 20% and 10%, respectively.

Titanium carbide and titanium diboride are used for refining the grains of aluminum alloys [26]. Due to good crystallographic compatibility with the matrix and some other mechanisms, these phases act as nucleation centers [27–29]. The microstructure and mechanical properties of an Al-4%Cu alloy with master alloys containing  $\text{TiB}_2$  particles was examined by Krishna N.N. et al. [30]. In addition to being grain refining agents, these particles—if added in sufficient quantity—can act as reinforcement. The introduction of  $\text{TiB}_2$  hardening particles in the Al-4%Cu alloy resulted in an increase in yield strength under tension. Similar results were obtained by other researchers [31,32].  $\text{TiB}_2$  particles used for modifying aluminum alloys are particularly attractive as  $\text{TiB}_2$  particles have high hardness and conductivity [33]. In contrast to SiC particles,  $\text{TiB}_2$  does not react with aluminum, therefore the formation of unstable products at the particle-matrix interface can be avoided with their use [34–38].

Thus, titanium diboride particles can be used to effectively manage the properties of aluminum alloys. However, introducing nonmetallic particles into the melt is challenging due to their agglomeration and non-uniform distribution in an ingot structure. To address this concern, various kinds of external actions on a metal melt are used. Many studies have examined the effects of ultrasound [12,39] and electromagnetic treatment [9,40] on aluminum melts. Vibration treatment is another method with external physical effects on a melt that are applied for improving the microstructure and, therefore, mechanical properties of aluminum alloys. Vibration treatment is an economical and simple method to control the melt and solidification. Vibration treatment provides excellent performance and energy consumption is reasonable.

However, issues related to the simultaneous effect of vibration treatment and modifying particles on the changes in structure and the improvement in mechanical properties of aluminum alloys are not well studied. The aim of this work was to study the combined effect of additions and vibration treatment on the as-cast structure and mechanical properties of an Al-Si aluminum alloy.

## 2. Materials and Experimental Procedure

A bespoke vibrating table was used to perform the vibration treatment. A356 aluminum alloy (United Company RUSAL Plc, Krasnoyarsk, Russia) was used as a matrix alloy, being a typical casting alloy for the automotive industry. Materials obtained using self-propagating high-temperature synthesis (SHS) from the Al-Ti-B powder system were applied as master alloys for modifying the aluminum structure.

To conduct SHS, the following powders were used: titanium powder (POLEMA, Tula, Russia; average particle size 100  $\mu\text{m}$ ), aluminum powder (United Company RUSAL Plc, Shelekhov, Russia; average particle size 80  $\mu\text{m}$ ), and amorphous boron powder (AVIABOR JSC, Dzerzhinsk, Russia; average particle size 800 nm). The preparation of the Al-Ti-B batch mixture for the SHS-process was implemented as follows. Titanium and boron powders were blended in a stoichiometric ratio of 69/31 wt%. Aluminum powder was added to the mixture in an amount of 50 wt%. From the obtained powder mixtures, samples with a diameter and a height of 40 mm were compacted at a pressure of 170 MPa. The compact was placed in a 3-L SHS reactor. After vacuum evacuation of the working chamber,

the reactor volume was filled with argon up to a pressure of 1.5 MPa. The SHS process was initiated locally using a molybdenum spiral. We produced composite master Al-TiB<sub>2</sub> system alloys that were used for alloy modification.

The experiment methodology for vibration treatment and master alloy introduction into an aluminum melt was implemented as follows: the charge of an A356 alloy ( $\approx 1$  kg) was placed in a crucible located in a melting enclosed-type furnace at a furnace temperature of 800 °C. The alloy was melted and kept in the furnace for at least 1 hour. Then, the crucible was removed from the furnace and the molten metal was poured at a temperature of 700 °C in a preheated chill mold with a cylindrical cavity (diameter 30 mm, height 110 mm), which was located on a vibrating table (Figure 1).

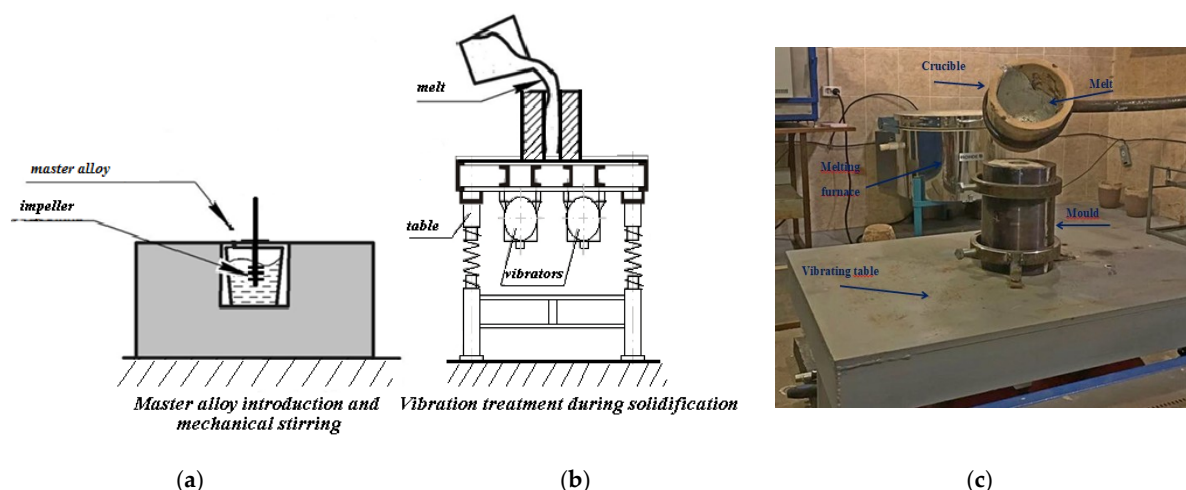


**Figure 1.** Scheme of vibration treatment on the melt. (a) master alloy introduction and mechanical stirring, (b) vibration treatment during solidification, (c) illustration of experimental apparatus for the mechanical vibration during the casting process.

To assess the integrated effect of modification and vibration treatment, another experiment was carried out. The Al-TiB<sub>2</sub> master alloy (0.5 wt%) was introduced into the A356 aluminum melt, after which the vibration treatment was applied. A special mixing device was used to uniformly distribute the master alloy (SHS materials) into the melt volume. A detailed description of the mixing device is provided by Vorozhtsov S. et al. [41]. The mixing was carried out for 30 s with subsequent casting into a steel chill mold located on the vibrating table.

A vibration frequency was 60 Hz and the processing time was at least 15 min (until complete crystallization of the melt). For a comparative assessment, samples without master alloy introduction and vibration treatment were also cast.

The 5 × 5 mm samples were cut from the center of the cylindrical casting and subjected to mechanical grinding and polishing. Anodizing was used to obtain color images of the grains and was performed using a 5% solution of HBF<sub>4</sub> with a voltage of 20 V and a current of about 1 A for 30 s. The grain size was evaluated by the random secant method, with no less than 300 measurements for each sample.

The structure of the obtained castings was studied using optical microscopy using a microscope Olympus GX-71 (Olympus Scientific Solutions Americas, Waltham, MA, USA) and by scanning electron microscopy (SEM) using electron microscopy Quanta 200™ 3D microscope (FEI Company, Thermo Fisher Scientific, Waltham, MA, USA). Mechanical tests were performed on an Instron® 3369 universal testing machine (Instron®, ITW Test & Measurement group, Norwood, MA, USA). Tensile specimens were in the form of flat blades with a working length of 25 mm and a cross-section of 1 × 5 mm. For each alloy, three tensile specimens were used.

### 3. Results and Discussion

The presence of inclusions in the solidification process under vibration and ultrasound has received considerable attention [42,43]. These inclusions can provide additional centers of solidification under certain conditions, so the additional effects of vibration on this process are of interest. The Al-TiB<sub>2</sub> master alloy used in this study has a structure as shown in Figure 2. A detailed analysis of structure formation and phase composition for such master alloys is provided elsewhere [44].

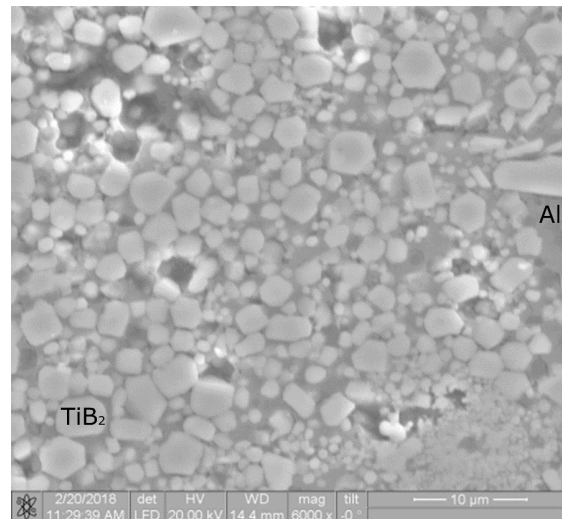


**Figure 2.** Structure of the Al-TiB<sub>2</sub> master alloy.

The average particle size of titanium diboride in the master alloy was about 3–5  $\mu\text{m}$ . It was easy to introduce the obtained master alloy into the melt due to the good separation of the particles by the aluminum matrix.

Gao Q. et al. [45] studied the formation of TiB<sub>2</sub> particles in the Al-4.5 wt.% Cu alloy in situ with introducing KBF<sub>4</sub> simultaneously with ultrasonic treatment. The authors found that titanium diboride particles mainly formed along the boundaries of aluminum grains and produced agglomerates, whose size was commensurate with that of aluminum grains. This alloy structure has a negative impact on its properties. As such, using composite master alloys, where TiB<sub>2</sub> particles are separated by a metal matrix (Al), is more efficient than the formation of titanium diboride in situ in an aluminum melt.

The microstructures of A356 aluminum alloys with and without 0.5 wt% titanium diboride addition (before and after vibration treatment) are presented in Figure 3.

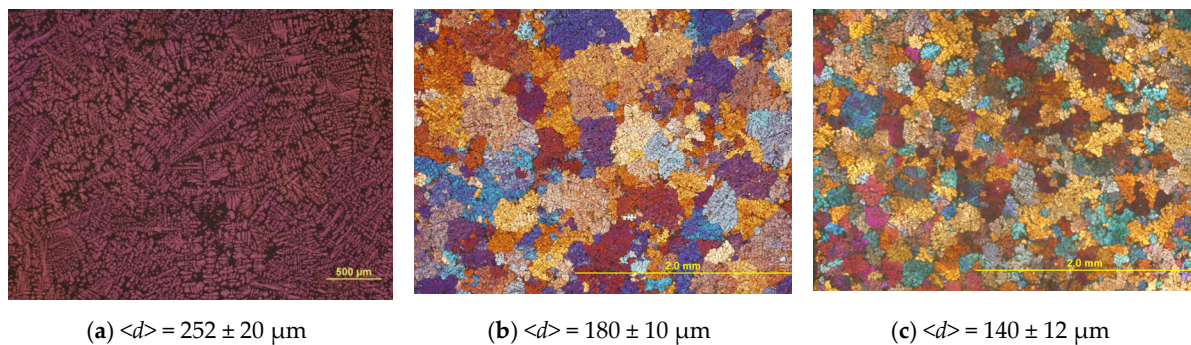


**Figure 3.** Microstructure of A356 aluminum alloy: (a) initial A356 alloy, (b) A356 alloy after vibration, and (c) A356 + 0.5 wt% TiB<sub>2</sub> after vibration treatment.

The microstructures of the A356 samples demonstrated that, during vibration treatment, significant structural changes occurred. This was reflected in the decreasing average grain size ( $\langle d \rangle$ ) of  $180 \mu\text{m}$  compared to that of the initial A356 alloy of  $252 \mu\text{m}$ .

The combined effect of  $\text{TiB}_2$  particles and vibration treatment of the melt considerably affected the grain size. There was a decrease in the average grain size of  $252 \pm 20 \mu\text{m}$  (initial A356 alloy) to  $140 \pm 12 \mu\text{m}$  ( $\text{A356} + 0.5 \text{ wt}\% \text{TiB}_2$  after vibration treatment). The decrease in grain size appears to be associated with the presence of additional crystallization centers.

The main purpose of vibration treatment of the melt is to reduce the chemical and structural heterogeneity of solidified alloys, as well as microsegregation. The results show that applying vibration to the A356 aluminum melt actually led to a significant structural refinement. The structure of the alloy transformed from dendrite to fine-grained. We found that the average grain size after the vibration treatment was  $180 \pm 10 \mu\text{m}$ . The probable reason for this finding is the fragmentation of dendrites and the distribution of the fragments via vibration-induced flows in the liquid and slurry volume, effectively leading to grain multiplication. Thus, vigorous mixing of the melt in the liquid and slurry parts of the casting is the main cause of changes in the ingot structure obtained after the vibration treatment.

The effects of vibration on the melt influence the final microstructure due to two principal mechanisms: (1) creation of periodic tension-pressure forces and (2) forced convection in the molten alloy [46,47]. Both affect the origin and growth of grains in the solidifying alloy. The vibration energy generates waves in the liquid alloy. Periodic tension-pressure forces are induced in the liquid elements as these waves pass. The vibration energy results in forced convection in the liquid. The flows caused by vibration affect the dendrite structures and lead to their destruction. When dendrites are destroyed, their parts collide with others, leading to their destruction as well. The nuclei are separate fragments of the dendrites for the creation of new grains during the alloy solidification [48]. Thus, vibration treatment significantly affects the formation of the alloy structure, with titanium diboride particles serving as additional centers of crystallization and contributing to the structure refinement [49,50].

Mechanical tensile testing of the A356 aluminum alloy and its variant (Figure 4) showed an increase in yield strength from  $67 \pm 6$  to  $121 \pm 7 \text{ MPa}$  after vibration treatment of the A356 alloy, whereas the tensile strength remained unchanged at  $182 \pm 7 \text{ MPa}$  and the elongation dropped two times.

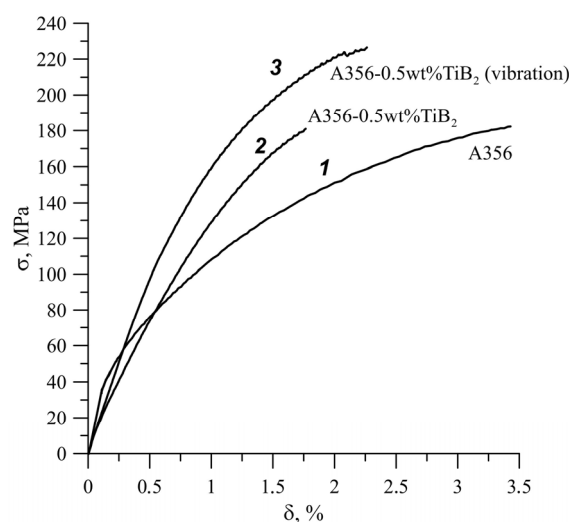


**Figure 4.** Mechanical properties of A356 aluminum alloy and aluminum-based composite alloys, before and after vibration treatment. (1) A356 alloy; (2) A356 alloy after vibration treatment; and (3) A356 + 0.5 wt%  $\text{TiB}_2$  after vibration treatment.

The introduction of 0.5 wt% titanium diboride particles with subsequent vibration treatment of the melt helped to improve the tensile test properties: yield strength increased to  $151 \pm 7 \text{ MPa}$  and

tensile strength to  $227 \pm 10$  MPa with a small decrease in the plasticity compared with the initial A356 alloy. Table 1 presents mechanical properties of the A356 alloy before and after vibration treatment.

**Table 1.** Mechanical properties of an initial A356 alloy and composites based on it, containing titanium diboride particles before and after vibration treatment.

Alloy	$\sigma_{0.2}$ (MPa)	$\sigma_B$ (MPa)	$\delta$ (%)
A356 alloy	$67 \pm 6$	$182 \pm 8$	$3.4 \pm 0.2$
A356 alloy after vibration	$121 \pm 7$	$182 \pm 7$	$1.7 \pm 0.1$
A356 + 0.5 wt% TiB <sub>2</sub> after vibration	$151 \pm 7$	$227 \pm 10$	$2.3 \pm 0.2$

The increase in composite strength characteristics compared with the initial A356 alloy may be related to the presence of structure heterogeneities that significantly affected the final mechanical properties of the materials. The mechanical properties were apparently formed due to the contribution of two mechanisms resulting from the presence of titanium diboride particles in the material structure. In the first case, the mechanism was due to the influence of the hardening particles on material properties (composite strengthening). The Hall-Petch law, as the second mechanism, appeared to be applicable in response to reducing a grain size of composites (A356 + 0.5 wt% TiB<sub>2</sub>) from  $252 \pm 20$   $\mu\text{m}$  to  $140 \pm 12$   $\mu\text{m}$  after the vibration treatment (in comparison with an initial alloy).

We observed an improvement in elastic and plastic characteristics with the introduction of 0.5 wt% TiB<sub>2</sub>. The simultaneous increase in the elastic and plastic characteristics can be explained by a more uniform deformation of the material due to the introduced particles. Belov N.A. [51] suggested that the introduction of particles into the grain body can lead to the deviation of a potential crack from the grain boundary into its volume, and to a greater involvement of the aluminum matrix in the process of deformation and fracture. Uniformly distributed particles can produce maximum plastic deformation of the matrix during crack propagation [51] and prevent the formation of main cracks [52]. A large number of particles can increase the density of interphase boundaries in the structure, reducing the role of grain boundaries as stress concentrators. As a result of the influence of all factors, the fracture mode of the alloy varied from intergranular to transgranular, leading to an increase in fracture toughness, as shown in Figure 5. The proposed hypothesis is in good agreement with the data obtained using the scanning electron microscope. We observed microparticles of titanium diboride uniformly distributed over the volume of the material in the structure of A356 + 0.5 wt% TiB<sub>2</sub> materials.

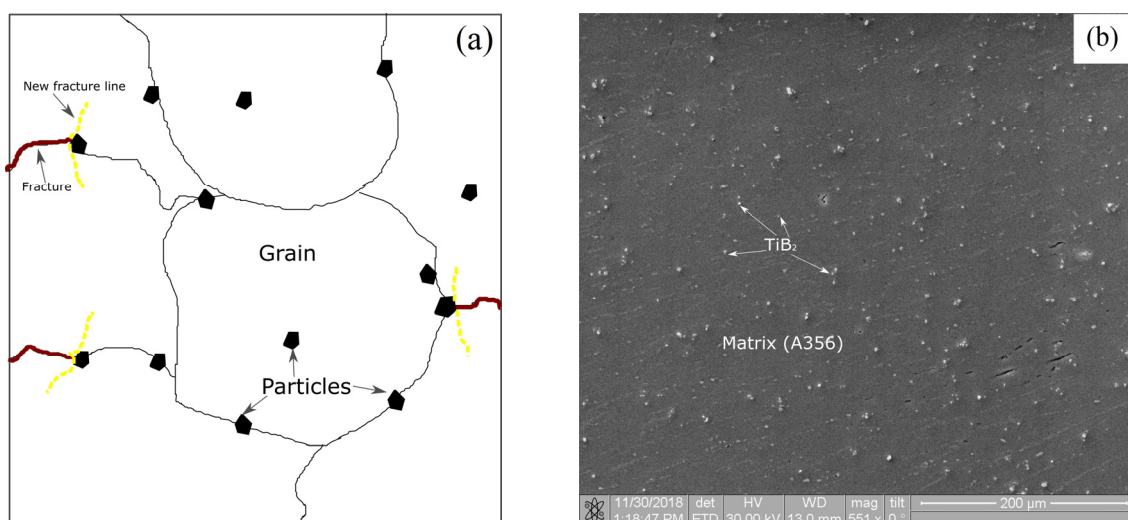


**Figure 5.** (a) Schematic design of the strengthening mechanism of aluminum alloys with the introduction of TiB<sub>2</sub> particles and (b) SEM image of the structure of the alloy A356 + 0.5 wt% TiB<sub>2</sub>.

#### 4. Conclusions

The study of the structure formation processes and properties of aluminum alloys in the vibration treatment and the introduction of a modifier, as composite master alloys, allowed us to evaluate the degree of changes in aluminum alloy properties. Elastic vibrations resulting from vibration treatment contributed to a crystal dispersion that appears into the melt. This led to the formation of equiaxed grains and an increase in the yield strength. The introduction of a modifying master alloy into the Al-TiB<sub>2</sub> system further refined the alloy structure, increasing the tensile strength up to 227 ± 10 MPa.

In summary, vibration treatment caused the fragmentation of crystalline grains and the reduction of columnar zones in casts. The formation of relatively large-scale melt flow causes temperature equalization in the liquid volume and the formation of transport processes of solid-phase fine-dispersed particles, a growth of crystal nucleation, and dispersed crystals. The increase in the amount of fine-dispersed phase and the transport of these particles by acoustic flows led to the formation of a more uniform fine-grained texture of solidified ingot.

**Author Contributions:** The manuscript was written by V.V.P. (Vladimir V. Promakhov) and I.A.Z. and V.V.P. (Vladimir V. Platov) designed and planned the experiments and microstructure studies. Mechanical properties tests were performed by M.G.K. and A.P.K., and A.B.V. was responsible for the project management.

**Funding:** Russian Science Foundation: 17-13-01252.

**Acknowledgments:** The research was performed with the financial support of a grant from the Russian Science Foundation (project No. 17-13-01252).

**Conflicts of Interest:** The authors declare no conflict of interest. The funders had no role in the design of the study; in the collection, analyses, or interpretation of data; in the writing of the manuscript, or in the decision to publish the results.

#### References

1. Kocatepe, K.; Burdett, C.F. Effect of low frequency vibration on macro and micro structures of LM6 alloys. *J. Mater. Sci.* **2000**, *35*, 3327–3335. [[CrossRef](#)]
2. Zhukov, I.; Promakhov, V.; Vorozhtsov, S.; Kozulin, A.; Khrustalyov, A.; Vorozhtsov, A. Influence of Dispersion Hardening and Severe Plastic Deformation on Structure, Strength and Ductility Behavior of an AA6082 Aluminum Alloy. *JOM* **2018**, *70*, 2731–2738. [[CrossRef](#)]
3. Li, C.L.; Mei, Q.S.; Li, J.Y.; Chen, F.; Maa, Y.; Meia, X.M. Hall-Petch relations and strengthening of Al-ZnO composites in view of grain size relative to interparticle spacing. *Scr. Mater.* **2018**, *153*, 27–30. [[CrossRef](#)]
4. Yoshitake, Y.; Yamamoto, K.; Sasaguri, N.; Era, H. Grain refinement of Al-2%Cu alloy using vibrating mold. *Int. J. Metalcast.* **2018**, 1–8. [[CrossRef](#)]
5. Abu-Dheir, N.; Khraisheh, M.; Saito, K.; Male, A. Silicon morphology modification in the eutectic Al-Si alloy using mechanical mold vibration. *Mater. Sci. Eng.* **2005**, *393*, 1–2. [[CrossRef](#)]
6. Vorozhtsov, S.; Kudryashova, O.; Promakhov, V.; Dammer, V.; Vorozhtsov, A. Theoretical and Experimental Investigations of the Process of Vibration Treatment of Liquid Metals Containing Nanoparticles. *JOM* **2016**, *68*, 3094–3100. [[CrossRef](#)]
7. Kotadia, H.R.; Qian, M.; Eskin, D.G.; Das, A. On the microstructural refinement in commercial purity Al and Al-10wt% Cu alloy under ultrasonication during solidification. *Mater. Des.* **2017**, *132*, 266–274. [[CrossRef](#)]
8. Wang, G.; Wang, Q.; Easton, M.A.; Dargusch, M.S.; Qian, M.; Eskin, D.G.; StJohn, D.H. Role of ultrasonic treatment, inoculation and solute in the grain refinement of commercial purity aluminium. *Sci. Rep.* **2017**, *7*, 1–9. [[CrossRef](#)]
9. Robles Hernández, F.C.; Sokolowski, J.H. Comparison among chemical and electromagnetic stirring and vibration melt treatments for Al-Si hypereutectic alloys. *J. Alloys Compd.* **2006**, *426*, 205–212. [[CrossRef](#)]
10. Mizutani, Y.; Tamura, T.; Miwa, K. Effect of Electromagnetic Vibration Frequency and Temperature Gradient on Grain Refinement of Pure Aluminum. *Mater. Trans.* **2007**, *48*, 538–543. [[CrossRef](#)]
11. Ghadimi, H.; Hossein Nedjhad, S.; Eghbali, B. Enhanced grain refinement of cast aluminum alloy by thermal and mechanical treatment of Al-5Ti-B master alloy. *Trans. Nonferrous Met. Soc. China* **2013**, *23*, 1563–1569. [[CrossRef](#)]

12. Zhukov, I.; Promakhov, V.; Dubkova, Y.; Matveev, A.; Ziatdinov, M.; Zhukov, A. Al-Ti-B4C materials obtained by high-temperature synthesis and used as a master-alloy for aluminum. *MATEC Web Conf.* **2018**, *243*, 00010. [[CrossRef](#)]
13. Vorozhtsov, S.A.; Eskin, D.G.; Tamayo, J.; Vorozhtsov, A.B.; Promakhov, V.V.; Averin, A.A.; Khrustalyov, A.P. The application of external fields to the manufacturing of novel dense composite master alloys and aluminum-based nanocomposites. *Metall. Mater. Trans. A* **2015**, *46*, 2870–2875. [[CrossRef](#)]
14. Taghavi, F.; Saghafian, H.; Kharrazi, Y.H.K. Study on the effect of prolonged mechanical vibration on the grain refinement and density of A356 aluminum alloy. *Mater. Des.* **2009**, *30*, 1604–1611. [[CrossRef](#)]
15. Chirita, G.; Stefanescu, I.; Soares, D.; Silva, F.S. Influence of vibration on the solidification behaviour and tensile properties of an Al–18 wt% Si alloy. *Mater. Des.* **2009**, *30*, 1575–1580. [[CrossRef](#)]
16. Jiang, W.; Chen, X.; Wang, B.; Fan, Z.; Wu, H. Effects of vibration frequency on microstructure, mechanical properties, and fracture behavior of A356 aluminum alloy obtained by expendable pattern shell casting. *Int. J. Adv. Manuf. Tech.* **2016**, *83*, 167–175. [[CrossRef](#)]
17. Zhao, Z.; Fan, Z.; Dong, X.; Tang, B.; Pan, D.; Li, J. Influence of mechanical vibration on the solidification of a lost foam cast 356 alloy. *China Foundry.* **2010**, *7*, 24–29.
18. Limmaneevichitr, C.; Pongananpanya, S.; Kajornchaiyakul, J. Metallurgical structure of A356 aluminum alloy solidified under mechanical vibration: An investigation of alternative semi-solid casting routes. *Mater. Des.* **2009**, *30*, 3925–3930. [[CrossRef](#)]
19. Fisher, T.P. Effects of vibrational energy on the solidification of aluminium alloys. *Br. Foundryman* **1973**, *66*, 71–84.
20. Mishra, S.S.; Sahu, S.S.; Ray, V. Effect of mold vibration on mechanical and metallurgical properties of Al-Cu alloy. *IJTRE* **2015**, *3*, 131–134.
21. Taghavi, F.; Saghafian, H.; Kharrazi, Y.H.K. Study on the ability of mechanical vibration for the production of thixotropic microstructure in A356 aluminum alloy. *Mater. Des.* **2009**, *30*, 115–121. [[CrossRef](#)]
22. Gencalp, S.; Saklakoglu, N. Effects of Low-Frequency Mechanical Vibration and Casting Temperatures on Microstructure of Semisolid AlSi<sub>8</sub>Cu<sub>3</sub>Fe Alloy. *Arab. J. Sci. Eng.* **2012**, *37*, 2255–2267. [[CrossRef](#)]
23. Gencalp, S.; Saklakoglu, N. Semisolid microstructure evolution during cooling slope casting under vibration of A380 aluminum alloy. *Mater. Manuf. Process.* **2010**, *25*, 943–947. [[CrossRef](#)]
24. Kumar, S.; Tewari, S.P. Effect of vibration on mechanical properties of A356 aluminum alloy casting. *IJMPERD* **2015**, *5*, 75–80.
25. Selivorstov, V.; Dotsenko, Y.; Borodianskiy, K. Influence of Low-Frequency Vibration and Modification on Solidification and Mechanical Properties of Al-Si Casting Alloy. *Materials* **2017**, *10*, 560. [[CrossRef](#)] [[PubMed](#)]
26. Napalkov, V.I. *Alloying and Modifying Aluminum and Magnesium*, National University of Science and Technology; MISiS: Moscow, Russia, 2002; ISBN 5-87623-100-2.
27. Jones, G.P.; Pearson, J. Factors affecting the grain-refinement of aluminum using titanium and boron additives. *Metall. Trans. B.* **1976**, *7*, 223–234. [[CrossRef](#)]
28. Brodova, I.G.; Popel, P.S.; Barbin, N.M.; Vatolin, N.A. *Original Melts as a Basis for the Formation of the Structure and Properties of Aluminum Alloys*; Ekaterinburg UrO RAN: Ekaterinburg, Russia, 2005; ISBN 5-7691-1609-9.
29. Antonio, J.A.M.; Lfo, L.F.M. Grain refinement in aluminum alloyed with titanium and boron. *Metall. Mater. Trans. B* **1971**, *2*, 465–471. [[CrossRef](#)]
30. Krishna, N.N.; Sivaprasad, K.; Susila, P. Strengthening contributions in ultra-high strength cryorolled Al–4%Cu–3%TiB<sub>2</sub> in situ composite. *Trans. Nonferr. Met. Soc. Ch.* **2014**, *24*, 641–647. [[CrossRef](#)]
31. Krishna, N.N.; Sivaprasad, K. High temperature tensile properties of cryorolled Al–4%Cu–3%TiB<sub>2</sub> in-situ composites. *Trans. Indian Inst. Met.* **2011**, *64*, 63–66. [[CrossRef](#)]
32. Mandal, A.; Maiti, R.; Chakraborty, M.; Murty, B.S. Effect of TiB<sub>2</sub> particles on aging response of Al–4Cu alloy. *Mater. Sci. Eng. A* **2004**, *386*, 296–300. [[CrossRef](#)]
33. Wu, S.Q.; Zhu, H.G.; Tjong, S.C. Wear Behavior of In Situ Al-Based Composites Containing TiB<sub>2</sub>, Al<sub>2</sub>O<sub>3</sub>, and Al<sub>3</sub>Ti Particles. *Metall. Mater. Trans. A* **1999**, *30A*, 243–247. [[CrossRef](#)]
34. Smith, A.V.; Chung, D.D.L. Titanium diboride particle-reinforced aluminium with high wear resistance. *J. Mater. Sci.* **1996**, *31*, 5961–5973. [[CrossRef](#)]
35. Zhukov, I.A.; Ziatdinov, M.H.; Vorozhtsov, A.B.; Zhukov, A.S.; Vorozhtsov, S.A.; Promakhov, V.V. Self-propagating high-temperature synthesis of Al and Ti borides. *Rus. Phys. J.* **2016**, *59*, 1324–1326. [[CrossRef](#)]

36. Yoshida, W.; Kobashi, M.; Kanetake, N. Synthesis of Fine Ceramic Particles in Molten Aluminum by Combustion Reaction. *Mater. Trans.* **2007**, *48*, 2374–2377. [[CrossRef](#)]
37. Hall, E.O. The brittle fracture of metals. *J. Mechan. Phys. Sol.* **1953**, *1*, 227–233. [[CrossRef](#)]
38. Khrustalyov, A.P.; Vorozhtsov, S.A.; Zhukov, I.A.; Promakhov, V.V.; Dammer, V.H.; Vorozhtsov, A.B. Structure and Mechanical Properties of Magnesium-Based Composites Reinforced with Nitride Aluminum Nanoparticles. *Rus. Phys. J.* **2017**, *59*, 2183–2185. [[CrossRef](#)]
39. Kudryashova, O.B.; Eskin, D.G.; Khrustalev, A.P.; Vorozhtsov, S.A. Ultrasonic Effect on the Penetration of the Metallic Melt into Submicron Particles and Their Agglomerates. *Rus. J. Non-Ferr. Met.* **2017**, *58*, 427–433. [[CrossRef](#)]
40. Haghayeghi, R.; Kapranos, P. Direct-chill casting of wrought Al alloy under electromagnetic and ultrasonic combined fields. *Mater. Lett.* **2013**, *105*, 213–215. [[CrossRef](#)]
41. Vorozhtsov, S.; Minkov, L.; Dammer, V.; Khrustalyov, A.; Zhukov, I.; Promakhov, V.; Vorozhtsov, A.; Khmeleva, M. Ex Situ Introduction and Distribution of Nonmetallic Particles in Aluminum Melt: Modeling and Experiment. *JOM* **2017**, *69*, 2653–2657. [[CrossRef](#)]
42. Lee, S.; Kwon, D.; Suh, D. Microstructure and fracture of SiC-particulate-reinforced cast A356 aluminum alloy composites. *Metall. Mater. Trans. A* **1996**, *27*, 3893–3901. [[CrossRef](#)]
43. Choi, H.; Jones, M.; Konishi, H.; Li, X. Effect of Combined Addition of Cu and Aluminum Oxide Nanoparticles on Mechanical Properties and Microstructure of Al-7Si-0.3Mg Alloy. *Metall. Mater. Trans. A* **2012**, *43*, 738–746. [[CrossRef](#)]
44. Zhukov, I.A.; Promakhov, V.V.; Matveev, A.E.; Platov, V.V.; Khrustalev, A.P.; Dubkova, Y.A.; Vorozhtsov, S.A.; Potekaev, A.I. Principles of structure and phase composition formation in composite master alloys of the Al-Ti-B/B<sub>4</sub>C systems used for aluminum alloy modification. *Rus. Phys. J.* **2018**, *60*, 2025–2031. [[CrossRef](#)]
45. Gao, Q.; Wu, S.; Lü, S.; Xiong, X.; Du, R.; An, P. Improvement of particles distribution of in-situ 5 vol.% TiB<sub>2</sub> particulates reinforced Al-4.5 Cu alloy matrix composites with ultrasonic vibration treatment. *J. Alloys Compd.* **2017**, *692*, 1–9. [[CrossRef](#)]
46. Campbell, J. Grain refinement of solidifying metals by vibration: A review. In Proceedings of the Solidification technology in the foundry and cast house, Coventry, UK, 15–17 September 1980; pp. 61–64.
47. Campbell, J. Effects of vibration during solidification. *Int. Mater. Rev.* **1981**, *2*, 71–106. [[CrossRef](#)]
48. Doherty, R.D. Comments on mechanical deformation of dendrites by fluid flow during the solidification of undercooled melts. *Scripta. Mater.* **2003**, *49*, 1219–1222. [[CrossRef](#)]
49. Vorozhtsov, S.A.; Promakhov, V.V.; Eskin, D.G.; Vorozhtsov, A.B.; Zhukov, I.A. The Use of Alumina and Zirconia Nanopowders for Optimization of the Al-Based Light Alloys. In Proceedings of the TMS 2015 Annual Meeting & Exhibition, Orlando, FL, USA, 15–19 March 2015; pp. 25–32.
50. Vorozhtsov, S.; Zhukov, I.; Promakhov, V.; Naydenkin, E.; Khrustalyov, A.; Vorozhtsov, A. The influence of ScF<sub>3</sub> nanoparticles on the physical and mechanical properties of new metal matrix composites based on A356 aluminum alloy. *JOM* **2016**, *68*, 3101–3106. [[CrossRef](#)]
51. Belov, N.A. Effect of eutectic phases on the fracture behavior of high-strength castable aluminum alloys. *Met. Sci. Heat Treat.* **1995**, *37*, 237–242. [[CrossRef](#)]
52. Chen, Z.; Wang, T.; Zheng, Y.; Zhao, Y.; Kang, H.; Gao, L. Development of TiB<sub>2</sub> reinforced aluminum foundry alloy based in situ composites—Part I: An improved halide salt route to fabricate Al-5 wt%TiB<sub>2</sub> master composite. *Mat. Sci. Eng. A* **2014**, *605*, 301–309. [[CrossRef](#)]

